

Stick-slip friction and nucleation dynamics of ultra-thin liquid films

I.S. Aranson¹, L.S. Tsimring², and V.M. Vinokur¹

¹ Argonne National Laboratory, 9700 South Cass Avenue, Argonne, IL 60439

² Institute for Nonlinear Science, University of California, San Diego, La Jolla, CA 92093-0402
(October 27, 2018)

We develop the theory for stick-slip motion in ultra-thin liquid films confined between two moving atomically-flat surfaces. Our model is based on hydrodynamic equation for the flow coupled to the dynamic order parameter field describing the “shear melting and freezing” of the confined fluid. This model successfully accounts for observed phenomenology of friction in ultra-thin films, including periodic and chaotic sequences of slips, transitions from stick-slip motion to steady sliding.

PACS: 62.20.Fe, 62.20.Qp, 68.60.-p

The nature of sliding friction is a fundamental physical problem of prime practical importance [1,2]. While the possibility to create low-friction surfaces and lubricant fluids has been ubiquitous for almost all engineering applications, it has become crucial for design of modern micro-miniature devices such as information storage and micro-electro mechanical systems, where low friction without stick-slip (or interrupted) motion is necessary.

Studies of friction between atomically flat mica surfaces separated by the ultra-thin layer of fluid lubricant have revealed a striking phenomenon [3]: in a certain range of experimental parameters the fluid exhibited solid-like properties, in particular, a critical yield stress leading to stick-slips similar to that in solid-on-solid dry friction process [4]. This behavior was attributed to the confinement-induced freezing of the lubricant and its recurring melting due to the increasing shear stress: as the fluid thickness is reduced to several molecular layers, it freezes, but when the shear stress exceeds some critical value, it melts (so-called “shear melting” effect). This behavior was confirmed by molecular dynamics simulations [5,6] that indicated ordering of the fluid due to confinement by the walls.

A quest for the quantitative description of the stick-slip lubricant dynamics motivated several theoretical works [7–9]. The important step has been made by Carlson and Batista [9] who proposed phenomenological constitutive relation connecting the frictional forces to velocity and coordinates via the order parameter-like state variable reflecting the degree of melting. This model successfully described some of the observed phenomenology of the experiment [3] and gave a new insight into the dynamics. Yet many important questions including the very mechanism of the onset of the stick-slip remain unresolved.

In this Letter we develop a theory of a stick-slip motion in an ultra-thin confined liquids based on the equation for the flow coupled to the equation for the order parameter (OP) for the melting transition in the presence of the shear stress. We propose that the shear melting is controlled by the stress tensor rather than the sliding velocity as assumed in [9]. Making use of the generalized

Lindemann criterion, we combine shear and thermodynamic melting within a unified description. Using this approach we describe the onset of the stick-slip motion as the function of the film thickness and determine the dynamic phase diagram. We demonstrate that random nucleation of droplets of the fluid phase during the motion leads to irregular temporal distribution of slip events.

Model. The flow of liquid lubricant has to satisfy the momentum conservation law:

$$\rho_0 \frac{Dv_i}{Dt} = \frac{\partial \sigma_{ij}}{\partial x_j}, \quad (1)$$

where v_i is a component of the fluid velocity, σ_{ij} is the stress tensor, $D/Dt = \partial_t + \mathbf{v}\nabla$ is the material derivative, and ρ_0 is the density of fluid. Assuming incompressibility we set $\rho_0 = 1$ and $\text{div} \mathbf{v} = 0$. We further assume that the lubricant satisfies Maxwell-type stress-strain relation:

$$\partial_t \sigma_{ij} + \eta \sigma_{ij} = \mu U_{ij} \quad (2)$$

where $U_{ij} = \partial v_i / \partial x_j + \partial v_j / \partial x_i$ is the shear strain rate, μ is the shear modulus, and η is the shear stress relaxation rate. Thus, the stress-strain relation includes both viscous flow and elastic restoring forces. The conventional shear viscosity is defined as $\nu = \mu/\eta$. To describe the dynamic phase transition between solid and fluid states we take into account that the stress relaxation rate η is itself a function of the physical state of the material quantified near the melting transition by the OP ρ which is defined in such a way that $\rho = 1$ corresponds to the solid state and $\rho = 0$ to the liquid state. Physical interpretation of the OP for various systems can be different, but for crystalline solids ρ can be related to the dislocation density. We restrict ourselves to the simplest dependence of the stress relaxation rate on ρ : $\eta = \eta_0(1 - \rho)$, $\eta_0 = \text{const}$. This choice assures that the Eq. (2) gives the standard Hook’s law for the pure solid ($\rho = 1$) and the standard viscous stress-strain relation for the Newtonian fluid with $\rho = 0$. We assume that the OP obeys the standard Ginzburg-Landau equation

$$\tau_0 \partial_t \rho = l^2 \nabla^2 \rho - \rho(1 - \rho)(\delta - \rho) \quad (3)$$

where τ_0 and l are the characteristic time and length correspondingly; l should be of the order of the lattice constant a , and the characteristic time can be expressed through the sound velocity c_s , $\tau_0 \approx l/c_s$. Here δ is the control parameter proportional to the temperature T . Since the melting transition in the lubricating layer occurs under the out-of-equilibrium conditions, it is characterized by two critical temperatures, T_1 , corresponding to an absolute instability of the overcooled liquid and T_2 , the stability limit of the solid phase [10,11]. The conventional thermodynamic melting temperature, T_m , is confined between these limits: $T_1 < T_m < T_2$. The parameter δ is naturally expressed in the form

$$\delta = (T - T_1)/(T_2 - T_1) \quad (4)$$

Now we have to relate the solid instability temperature T_2 to the stress generated in the process of motion. To this end we notice first that in the absence of dynamic shear deformations the temperature T_2° can be estimated as $T_2^\circ = \tilde{c}_L^2 \mu a^3$, where a is the lattice constant for the solid crystalline state, μ is the shear modulus (we write everything in a scalar form for simplicity), and \tilde{c}_L^2 is the numerical factor (“Lindemann number”). Assuming independence of thermal fluctuations and shear, one can present a rms displacement field in a form:

$$\langle u^2 \rangle \simeq \frac{T}{\mu a} + \frac{\sigma^2}{\mu^2}, \quad (5)$$

where $\sigma \equiv \sigma_{xy}$ is the shear stress, and the first term in the rhs stands for the thermal average displacement, while the second term expresses the shear-induced displacement field. In writing Eq. (5) we hypothesize that the solid phase instability can stem not only from the thermal fluctuations, but also from the shear, generated by the mutual motion of the solid surfaces confining the lubricant. At zero physical temperature the instability can be caused by this shear only, this concept of *shear-induced melting* generalizes the hypothesis of the dynamic disorder-driven melting introduced in earlier work [12]. At the temperature T_2 the relation $u^2 = \tilde{c}_L^2 a^2$ holds, and we immediately obtain from Eq.(5)

$$T_2 = \tilde{c}_L^2 \mu a^3 - \sigma^2 a / \mu = T_2^\circ - \sigma^2 a / \mu \quad (6)$$

Substituting Eq. (6) into the expression for the control parameter δ Eq. (4) one derives in the first order

$$\delta = \delta_0 + \sigma^2 / \sigma_0^2 \quad (7)$$

where $\delta_0 = (T - T_1)/(T_2^\circ - T_1)$ and $\sigma_0 = \sqrt{\mu(T_2^\circ - T_1)/a\delta_0}$ has a meaning of the yield shear stress.

In the *thin layer approximation* we assume that the thickness of the lubricant layer h is small and neglect the dependence of the shear stress σ on the transverse coordinate z . We can also neglect the dependence of σ on the longitudinal coordinate x if the sample size L is

not very large. Indeed, if the “acoustic shear time” $\tau_a = L/c_s$ is much smaller then any characteristic time scale of the problem (e.g stick-slip time), the spatial variation of the stress is negligible, and the shear stress becomes the function of time only [14]. In this approximation after the integration over the area of the sample, Eq. (2) gives:

$$\sigma_t + \frac{\sigma \eta_0}{Lh} \int_0^L \int_0^h (1 - \rho) dx dz = \frac{\mu V}{h}, \quad (8)$$

where V is the relative velocity of the upper plate with respect to the bottom.

Now we can further simplify the OP dynamics. Since the walls favor the formation of the solid, the boundary conditions for OP read: $\rho(0) = \rho(h) = 1$, and the bulk variation of the OP are small as compared to 1. Let us seek the solution in a form

$$\rho(x, z, t) = 1 - A(x, t) \sin(\pi/hz) \quad (9)$$

where $A \ll 1$ is the slowly varying amplitude. Substituting Eq. (9) into Eq. (3) and making use of the standard orthogonality procedure leads to

$$A_t = A_{xx} + (\delta - 1 - \frac{\pi^2}{h^2}) A + \frac{8}{3\pi} (2 - \delta) A^2 - \frac{3}{4} A^3 \quad (10)$$

where $\delta = \delta_0 + \sigma^2$, and variable were rescaled as $x/l \rightarrow x, t/\tau \rightarrow t, \sigma_{xy}/\sigma_0 \rightarrow \sigma$. Accordingly, Eq. (8) yields:

$$\sigma_t + \frac{2\eta_0}{\pi L} \sigma \int_0^L A(x) dx = \frac{v_0}{h}, \quad (11)$$

where $v_0 = \mu V / \sigma_0$ is the normalized pulling velocity. Note that in the most of the dynamic friction experiments the pulling velocity \bar{V} does not coincide with the upper plate velocity V . In fact, the relation between the position of the upper plate x , friction force F , and the position of the spring (neglecting the mass of the spring and upper plate) is as follows: $F = k(\bar{V}t - X)$, where X is the horizontal position of the upper plate and k is the stiffness of the spring. Since $F \sim \sigma L$, and $V = dX/dt$, one immediately sees that exclusion of the plate velocity V results in the equation that is qualitatively the same as Eq. (11) but has renormalized v_0 and η_0 . Thus to simplify further discussion we will consider $V = \bar{V}$.

Stick-slip motion. First we discuss the spatially-uniform motion. In this case Eqs.(10),(11) become a pair of coupled ordinary differential equations (ODE). Above the melting temperature $\delta_0 > 1$, the solid phase of the lubricant is formed due to proximity-to-the-walls effect. In the experimentally relevant limit $\eta_0, v_0 \ll 1$ the abovementioned ODEs can be investigated analytically by the bifurcation analysis and the multi-scale technique with σ being a slow and A being a fast variable. Stick-slips are described by the limit cycle on the $\sigma - A$ plane. The transitions between different regimes are determined by the intersection of the manifold of

the slow motion $\frac{2\eta_0}{\pi}\sigma A = v_0/h$ and the fast motion $(\delta - 1 - \frac{\pi^2}{h^2}) + \frac{8}{3\pi}(2 - \delta)A - \frac{3}{4}A^2 = 0$. The transition from the stick-slip to sliding corresponds to the intersection of the slow motion manifold with the minimum of the fast motion manifold $\sigma = f(A)$, i.e. $d\sigma/dA = 0$. The limit cycle vanishes smoothly at the transition point if there is only one intersection of two manifolds, otherwise the cycle disappears abruptly with hysteresis.

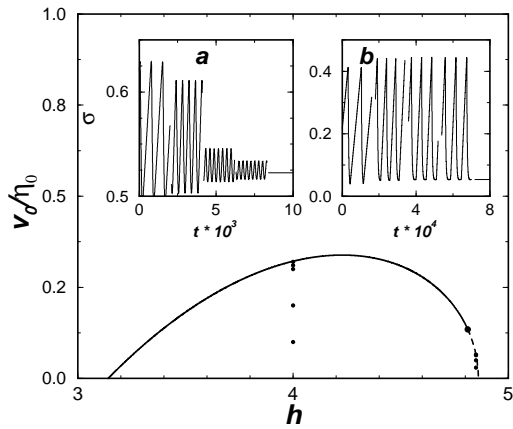


FIG. 1. Phase of lubrication regimes at $\delta_0 = 1.3$. Solid line indicates the continuous transition from stick-slip to sliding, and the dashed line corresponds to the hysteretic abrupt transition. Insets A,B show normalized shear stress σ vs time for $\eta_0 = 0.01$ at two different values of h corresponding to continuous and discontinuous transitions, and several values of v_0/η_0 approaching the transition line (dots in the main plot): $h = 4$, $v_0/\eta_0 = 0.1, 0.2, 0.3, 0.31, 0.32$ (A) and $h = 4.85$ $v_0/\eta_0 = 0.03, 0.05, 0.064, 0.0645, 0.065$ (B).

Figures 1,2 illustrate the transition from continuous sliding to the stick-slip motion. As one can see from Fig. 1, 2, stick-slip are possible only in relatively thin layers, while in the thick layers sliding is steady since the lubricant in the bulk is always in a fluid state. The critical thickness h_c is determined by the stability condition $d\sigma/dA = 0$: $h_c = \pi/\sqrt{\delta_0 - 1 + 64(2 - \delta_0)^2/27\pi^2}$. We find that for h close to h_c the transition from the stick-slip to sliding is always abrupt and has a hysteretic character (see Fig. 2 and Fig. 1, Inset B). For the parameters chosen, the “friction law” σ vs v_0 has a minimum, (Fig. 2, inset, curve 2) as common for a typical dry friction behavior [1]. For smaller δ_0 the transition is continuous (inset A in Fig. 1, curve 3 in Fig. 2, inset). For $h < h_0 = \pi$ the dry friction without stick slip occurs because the viscous friction force become larger then the dry friction one, curve 1 in Inset [13].

Nucleation. The above analysis presumed that the stick-slip happens simultaneously in the entire space, which is certainly not the case for large samples. It is natural to expect that the stick-slip occurs via series of

nucleation events when droplets of the liquid emerge in the solid phase and then expand and merge throughout the system. It is interesting to connect the nucleation dynamics in the systems with the lubricated friction with the creation of topological defects during rapid quench (“cosmological scenario”) [15–17]. Since in the stick phase the value of A is close to zero, the solid phase can be significantly “overheated” by the shear. For $A \ll 1$, integration of Eq. (10) yields

$$A \approx A_0 \exp \left(\int_0^t (-\epsilon + \sigma^2) dt \right), \quad (12)$$

where $\epsilon = 1 + \frac{\pi^2}{h^2} - \delta_0 > 0$. From Eq. (11), $\sigma \approx v_0 t/h + \sigma_0$, and A_0, σ_0 are the values of amplitude and stress in the beginning of stick phase. We restrict ourselves to the case $h \rightarrow h_c$, where $\sigma_0 \rightarrow 0$ and $A_0 = O(1)$. While σ is small, the amplitude A decays exponentially to very small values. It reaches a minimum $A_{min} = \exp(-2\epsilon^{3/2}h/3v_0)$ at $t_{min} = \epsilon^{1/2}h/v_0$. Then it starts slowly to grow and reaches the value $O(1)$ (slip event) at $t = t_m = \sqrt{3}t_{min}$. At $t_{min} < t < t_m$ the growthrate $-\epsilon + \sigma^2 > 0$, and therefore the lubricant is in an unstable (“overheated”) state. The overheated solid is very sensitive to fluctuations, e.g. to thermal noise. Small nuclei of liquid can appear and expand within the solid, resulting to an accelerated slip event. Since at the low noise level nucleation events have the probabilistic character, one can expect the spatio-temporal randomness of the slip events. At the higher level of the noise the slips become more regular because the number of nucleation sites increases and the overall effect of the noise is averaged out.

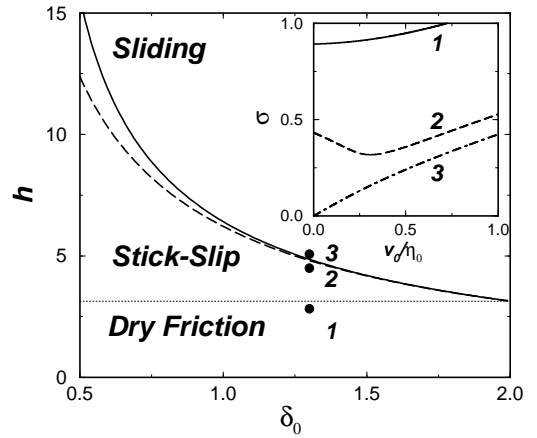


FIG. 2. Temperature (δ_0)-thickness (h) diagram. Above solid line (h_c) sliding occurs for arbitrary small velocity v_0 . Left of h_c stick-slips exist for $v_0 < v_c$, while the transition to sliding is abrupt with hysteresis between solid and dashed lines and smooth otherwise. Below dotted line (h_0) one has dry friction without stick-slips. Inset: shear stress σ (or friction force) vs sliding velocity v_0 in three different regions.

We studied Eqs. (10,11) numerically in a fairly large

domain, see Figs. 3,4. Since during the slip phase the shear stress rapidly drops, the domains do not necessary propagate through the entire system and in large systems one may observe “partial slips.” The random character of the nucleation process manifests itself in the non-periodicity of slips and local amplitude A .

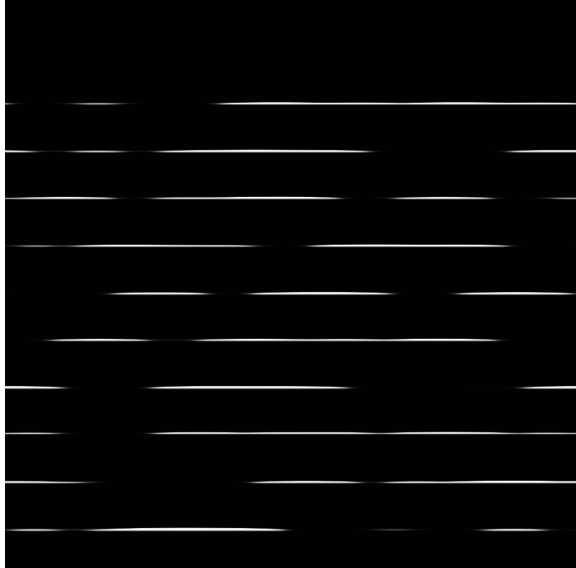


FIG. 3. Space-time plot of A for $\delta_0 = 1.1$, $h = 4$, $\eta = 0.01$, $v_0 = 0.0002$ in the system of length $L = 1000$. Black correspond to $A = 0$ (solid), white to $A = 1$ (liquid). Time progresses from top to bottom, total integration time 30000 dimensionless units. Uncorrelated noise with zero average and amplitude 10^{-16} is add on each time step and each grid point.

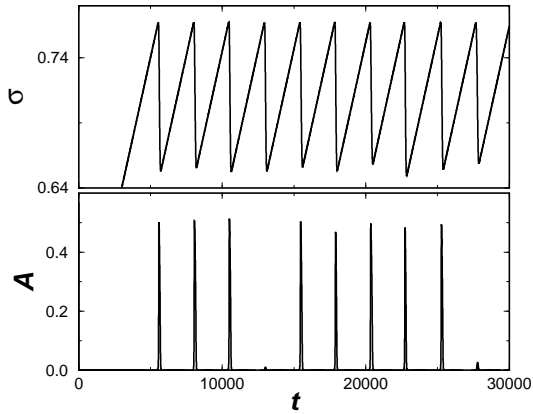


FIG. 4. σ and A at $x = L/2$ vs t for parameters of Fig. 3.

In conclusion, we have investigated the friction dynamics in ultra-thin liquid films. We have related the stick-slip behavior of thin liquid films to shear-induced melting and freezing processes. The developed approach allowed for the first time a quantitative description of dynamic nucleation effects leading to slip events. The proposed

theory can be applied to a wide range of phenomena including friction in nanoscale devices, friction on ice, granular materials [18] as well as depinning transitions of flux-line lattices in type-II superconductors, charge density waves and other structures driven through disorder [12]. Our model offers a description for the long-standing problem of the ultra-sound emition during the friction dynamics. This research is supported by the Office of the Basic Energy Sciences at the US DOE, grants W-31-109-ENG-38, DE-FG03-95ER14516, and DE-FG03-96ER14592

- [1] B.N.J. Persson, *Sliding Friction. Physical Principles and Applications*, Springer-Verlag, 1998
- [2] E. Meyer, R.M. Overney, K. Dransfeld, and T. Gyalog, *Nanoscience. Friction and Rheology on the Nanometer Scale*, World Scientific, 1998
- [3] H. Yoshizava and J. Israelachvili, *J. Phys. Chem.* **97**, 4128 (1993)
- [4] G. Hähner and N. Spencer, *Phys. Today* **22** (9), 22 (1998); T. Baumberger, P. Berthoud, and C. Caroli, *Phys. Rev. B* **60**, 3928 (1999);
- [5] P.A. Thompson and M.O. Robbins, *Phys. Rev. A* **41**, 6830 (1990); *Science* **250**, 792 (1990)
- [6] J.P. Gao, W.D. Luedtke, and U. Landman, *J. Chem. Phys.* **106**, 4309 (1997)
- [7] O. Braun, A.R. Bishop and J. Röder, *Phys. Rev. Lett.* **82**, 3097 (1999)
- [8] W. Zhong and D. Tomanek, *Europhys. Lett.* **15**, 887 (1991)
- [9] J.M. Carlson and A.A. Batista, *Phys. Rev. E* **53**, 4153 (1996).
- [10] L. Pietronero, in *Phonons: Theory and Experiments*, ed. P.Brüesch (Springer, Berlin, 1987), Vol. III, Chap. 8.
- [11] T.V. Ramakrishnan and M. Yousouff, *Phys. Rev. B* **19**, 2775 (1979)
- [12] A. E. Koshelev and V. M. Vinokur, *Phys. Rev. Lett.*, **73**, 3580 (1994)
- [13] Curves 1 and 2 of Fig. 2 are reminiscent of the generic behavior of lattices driven through random environment, near the depinning transition: curve 1 describes *elastic* depinning from weak disorder and curve 2 represents hysteretic depinning corresponding to the case of strong disorder, see e.g. V. M. Vinokur and T. Nattermann, *Phys. Rev. Lett.* **79**, 3471 (1997); M. C. Marchetti, A. Middleton, and T. Prellberg, *Phys. Rev. Lett.* **85**, 1104 (2000)
- [14] Validity of similar condition of isobaricity in the context of radiative condensation is discussed in detail by B. Meerson, *Rev. Mod. Phys.* **68**, 215 (1996), and I. Aranson, B. Meerson, P. Sasorov, *Phys. Rev. E* **52**, 948 (1995).
- [15] T.W.B. Kibble, *J. Phys. A: Math Gen* **9**, 1387 (1976)
- [16] W. H. Zurek, *Nature* **317**, 505 (1985); N.D. Antunes, L.M.A. Bettencourt, and W.H. Zurek, *Phys. Rev. Lett.* **82**, 2824, (1999).
- [17] I.S. Aranson, N.B. Kopnin and V.M. Vinokur, *Phys. Rev. Lett.* **83**, 2600 (1999)
- [18] W. Losert *et al*, *Phys. Rev. E* **61**, 4060 (2000)